

# Analysis of three-dimensional photonic crystals fabricated by the microexplosion method

Aaron Matthews<sup>a</sup>, Guangyong Zhou<sup>b</sup>, Min Gu<sup>b</sup>, and Yuri Kivshar<sup>a</sup>

<sup>a</sup>Nonlinear Physics Centre and Centre for Ultra-high bandwidth Devices for Optical Systems, Research School of Physical Sciences and Engineering, Australian National University, Canberra ACT 0200, Australia

<sup>b</sup>Centre for Micro-Photonics and Centre for Ultra-high bandwidth Devices for Optical Systems, Swinburne University of Technology, P.O. Box 218, Hawthorn Victoria 3122, Australia

## ABSTRACT

Fabrication of three-dimensional photonic crystals by the microexplosion techniques has recently been demonstrated by a number of groups. However, simple models which are currently used for characterizing the void-based photonic structures do not produce adequate results. Here, we suggest a new theoretical approach for analyzing the properties of the three-dimensional photonic crystals which allow to improve the results of the theoretical modeling of the photonic crystals created by the microexplosion method. In particular, we study the bandgap spectrum of the three-dimensional photonic crystals introducing a shell of a high-index material surrounding an air void in the face-centered-cubic lattice. This allows us to suggest an effective theoretical model which correlates very well with the properties of the microexplosion polymer photonic crystals produced experimentally. We also discuss some interesting effects observed in the fabricated photonic crystals which until now have not been understood due to the inadequacies of simple models.

**Keywords:** Microexplosion fabrication, 3D photonic crystals, Microexplosion modeling

## 1. INTRODUCTION

Ultrafast laser-driven microexplosion method was suggested almost ten years ago to generate air voids in a dielectric material. The method is based on a simple process when, by tightly focusing femtosecond laser beam into a solid transparent material, some material can be ejected near the focal point of the laser beam forming a void cavity surrounded by a region of more compressed material.<sup>1</sup> This microexplosion method was also proposed for the three-dimensional read-only optical data storage,<sup>2,3</sup> and later employed for the fabrication of three-dimensional periodic photonic structures.<sup>4-7</sup> Smooth void dots and void channels have been generated in glass<sup>4,5</sup> and polymer materials<sup>6-9</sup> being stacked to form two-dimensional (2D) or three-dimensional (3D) photonic-crystal structures. This technique provides a one-step method, and it does not require chemical post-processing allowing the fabrication of photonic crystals with a high degree of perfection.<sup>10</sup>

Compared with glass materials, polymer materials also have a low threshold to generate void dots and good index matching which has been a significant problem for the microexplosion technique in lithium niobate.<sup>11</sup> One more advantage to use photopolymers is the ability to infiltrate different materials into their pores, which is especially useful to create nonlinear elements. In particular, the infusion of liquid crystals and the implantation of quantum dots into photopolymer's voids may result in novel nonlinear structures for tunable photonic devices.

However, the modeling of the periodic structures produced by the microexplosion method is more difficult than the analysis of the periodic structures fabricated by other methods due to several factors. First, unlike the media of a single-atom-type such as silicon, the long-chain structure of polymers (e.g., urethane) does not compress or even react in a simple way to the physical compression. Second, unlike the deposition or etching methods the material compressed in the fabrication does not leave the crystal.

---

Aaron Matthews: E-mail: [afm124@rsphysse.anu.edu.au](mailto:afm124@rsphysse.anu.edu.au), Telephone: +61 2 6125 8277  
Guangyong Zhou: E-mail: [gzhou@swin.edu.au](mailto:gzhou@swin.edu.au), Telephone: +61 3 9214 5719

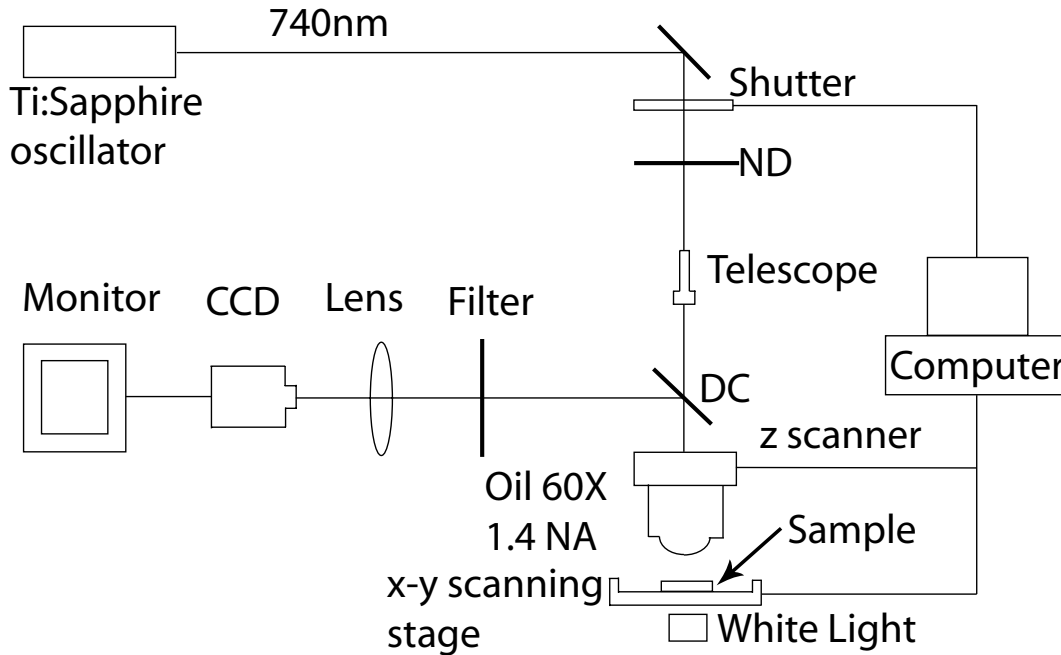


**Figure 1.** Schematic of the experimental setup for fabricating photonic crystals by the microexplosion method.

To understand the photonic crystals created from polymers by the microexplosion technique, first we need to understand the process by which they are created. We look at the fabrication process as well as the internal processes in the polymer. From this, we gain a better understanding how to model the resulting structure. There is a number of possible approaches to simulate numerically this system, and we discuss some of them. With an understanding of the polymer photonic crystals created by the microexplosion method, we can apply the ideas to other structures such as those involving the addition of an interfacial layer<sup>12-14</sup> and conjoined shells,<sup>15</sup> or the inverse structures created by shells in air.<sup>16</sup> We believe our studies may also provide a better understanding of the dispersion and density of states in these photonic crystals.

The paper is organized as follows. In Sec. 2 we present some of the experimental results and discuss the microexplosion method in more details, for the example of the periodic structures with the face-centered-cubic (fcc) lattice symmetry. Our theoretical results are presented in Sec. 3, where we discuss a novel approach to analyze the structures with a periodic lattice of voids. Finally, Sec. 4 present some discussions of the results and a summary of our work.

## 2. EXPERIMENTAL METHODS AND RESULTS

To fabricate the 3D photonic crystals, we use a transparent photosensitive polymer resin, optical adhesive NOA 63 (Norland Product Inc., USA). The resin is shaped into a thin film with a thickness of approximately  $100 \mu\text{m}$  with a standard cover slip on top of it and pre-cured by the use of a ultraviolet light.

The experimental setup is shown in Fig. 1, and it is similar to that described earlier.<sup>7</sup> A 740-nm light pulse of  $\sim 80$  fs is generated by a Tsunami femtosecond oscillator (Spectra-Physics, USA). The laser beam is then expanded by an inverse telescope system and tightly focused by a 1.45 numerical aperture, 60 $\times$  oil immersion objective. A shutter is used to control the laser light power, while a write-light source is used to illuminate the structure. The image of the structure is collected through the same objective and reflected by a dichromatic mirror to a CCD camera, so that the fabrication process can be in situ monitored. The sample is affixed to a 3D piezoelectric scanning system (PI, Germany) that is controlled by a computer.

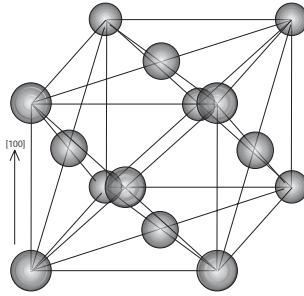


**Figure 2.** A unit cell of the face-centered-cubic lattice; the [100] direction is marked.

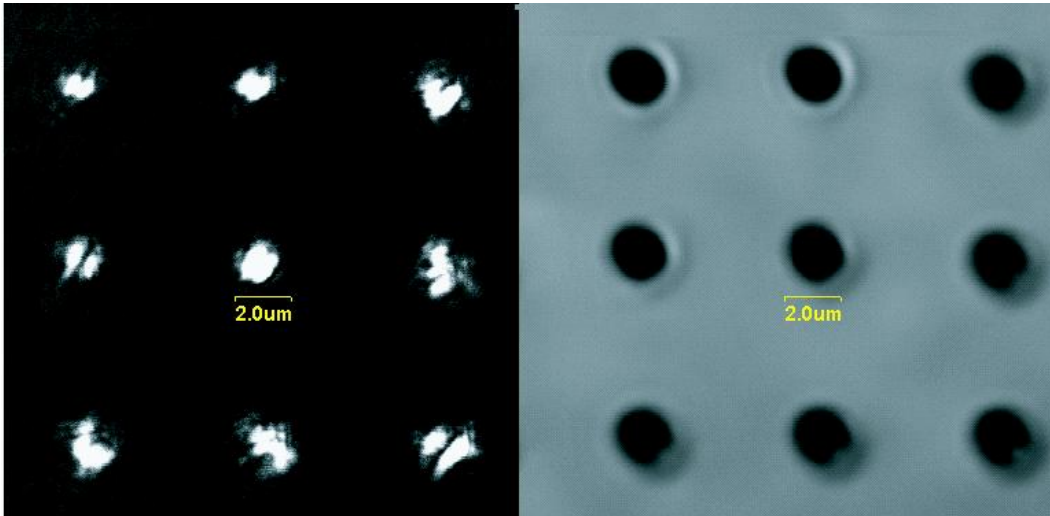


**Figure 3.** Experimental images of the voids produced by the microexplosion method. Left: the structure recorded by a confocal reflection microscope; right: the structure recorded by a confocal transmission microscope.

In order to generate voids in the polymer, the sample is kept still while the shutter is opened. Then the sample is moved to the next position while the shutter remains closed. By controlling the exposure time and power, we control the size of the void dots<sup>7</sup> and, therefore, control the filling factor of the fabricated photonic structure. The photonic crystals with the fcc symmetry are fabricated layer by layer. First, we fabricate the deepest layer, then the second deepest layer, and so on, so that the fabricated void dots do not interfere the later fabrication process. The start position of the first layer is calculated beforehand and it depends on the layer number and the lattice constant so that the first layer can be located at  $5 \mu\text{m}$  below the top surface.

Figure 2 shows schematically a unit cell of the fcc lattice. In the [100] direction of the parallel planes of the lattice points are fabricated in the form of a square lattice. These are built up with a periodicity of two, offset by the distance  $a/\sqrt{2}$  in the  $x$ -direction. Adjacent layers are separated by the distance  $a/\sqrt{2}$ . The structures consisting of 28 layers of void dots with the top layer  $5 \mu\text{m}$  below the surface have been fabricated by applying a power of 40 mW for an exposure time of 10 ms. The average diameter of the fabricated spherical void dots is approximately  $1.5 \mu\text{m}$ . Due to a spherical aberration caused by a slight refractive index mismatch between the polymer ( $n = 1.56$ ) and the immersion oil ( $n = 1.52$ ),<sup>17</sup> the void dots are slightly smaller at a larger depth. The light penetrates through the photonic crystals perpendicular to the polymer film for both the fabrication process and the infrared transmission spectra measurement but with a significant restriction in the stop gaps.

The uniformity of the voids is examined using a reflection confocal microscope (Fluoview, Olympus, Japan). Figure 3 shows an image of void dots with a spacing of  $3.46 \mu\text{m}$  recorded by a confocal reflection microscope

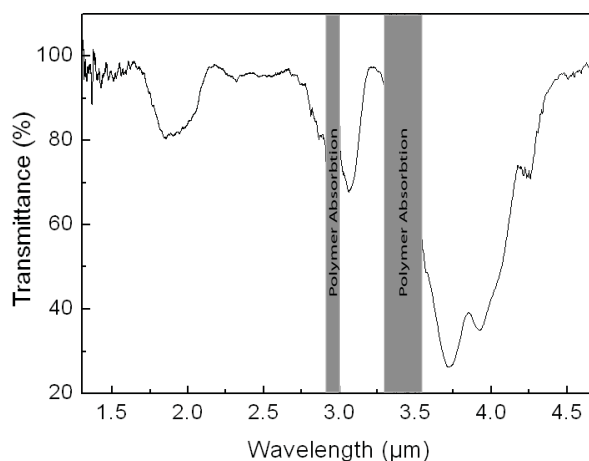


**Figure 4.** The transmission spectra for a 3D fcc lattice oriented in the [100] direction. The suppression in the main band gap is close to 75% which is an exceptionally good result for fabricated photonic crystals.

(left) and by a confocal transmission microscope (right). The strong reflection signal from the dots (see Fig. 3, left) indicates a high-refractive-index contrast between the fabricated and un-fabricated region, which verifies the generation of voids at the focal point.<sup>3</sup> The change in colour at the void edge (see Fig. 3, right) indicates a compression-based index change.

Uniformity of the fabricated structures of void dots is examined by measuring the transmission spectra. A Nicolet Nexus FTIR spectrometer is used to provide infrared light with the wavelength from 1  $\mu\text{m}$  to 5  $\mu\text{m}$  and a 32 $\times$ , NA 0.65 reflective objective (Reflechromat, Thermo Nicolet, Madison, WI, USA) is used to focus the light beam on the structure. The reflective objective provides an incident hollow light cone with an outer angle of 40 $^\circ$  and an inner angle of 15 $^\circ$  (which corresponds to 25 $^\circ$  and 10 $^\circ$  in the sample). Therefore, the measured spectrum is an average over the entire range of the incidence angles mentioned above. The curve in Fig. 4 shows the transmission spectrum of a 28-layer fcc structure stacked in the [100] direction with a lattice constant of 4.0  $\mu\text{m}$ . One can see that there is a wide trough from 3.6  $\mu\text{m}$  to 4.25  $\mu\text{m}$  with the maximum suppression rate of approximately 75%. To reduce the range of the incidence angle, an adjustable aperture is attached to the FTIR objective, resulting in a hollow light cone with an adjustable outer angle of incidence and an inner angle of 10 $^\circ$ .

To confirm that the wavelength of the fabricated photonic crystal is proportion to the lattice constant, we fabricate several fcc structures stacked in the [100] direction with different lattice constants.<sup>9</sup> As expected, all of the observed bandgaps shift to longer wavelengths as the lattice constant increases.

### 3. THEORETICAL ANALYSIS

The voids produced in this system are quite accurate, and it is simple to demonstrate the existence of a photonic bandgap in the periodic structures fabricated in polymers. However, other properties of such structures are less known, and the straightforward application of the numerical methods does not correlate with the experimental data.

Indeed, in most of the photonic-crystal fabrication systems we can assume that the refractive index remains homogenous in the regions occupied by the dielectric. This is demonstrated well in the structures fabricated by deposition, photopolymerisation and etching processes; but in the structures fabricated by the microexplosion method we do not remove the material from the system, but simply move it away from the focal point into the surrounding area creating a void. This excessive material is observed in Fig. 3 in the form of a ring surrounding the void.

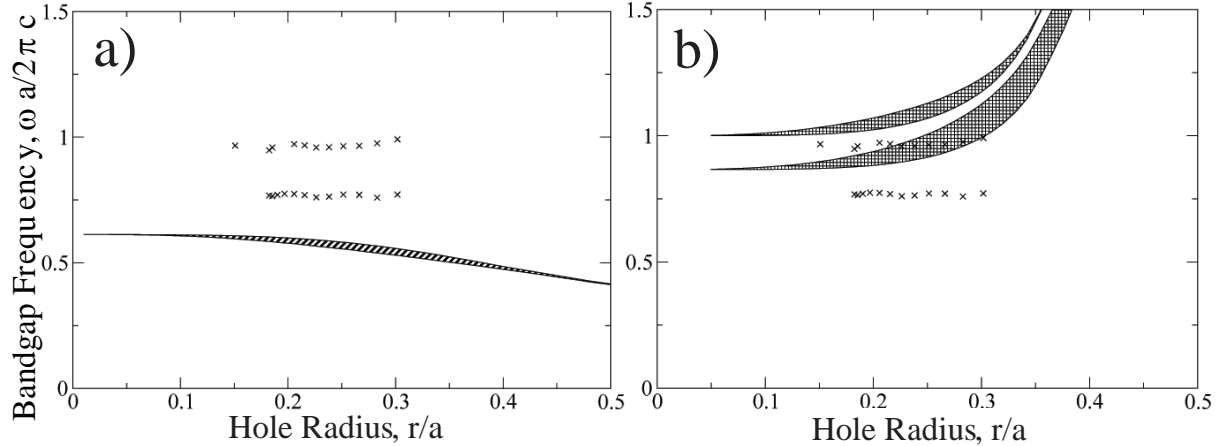


**Figure 5.** (a) The lowest bandgap for the 3D fcc lattice of voids calculated with the assumption of a homogenous refractive index  $n = 1.56$  of the unmodified NOA63 photopolymer. (b) Same for the 3D fcc lattice with a constant volumetric average of the refractive index.

If the structure fabricated by the microexplosion method is simulated as a homogenous system, as presented in Fig. 5(b), the results correlate very poorly with the experimental data. This confirms our assumption about the inherent difference between our system and the photonic crystals fabricated by other methods. And, in order to model accurately our system, we should include some effects describing the properties of the processes involved in the void fabrication.

The compression of a polymer requires more in depth study of the material properties than for other materials and methods. In a polymer, long chains compress and exert a reactive force as they attempt to return to their original orientation. They also produce a frictional damping as the molecules move past each other which slows the compression progress. This knowledge can be combined into a control system with the explosion modeled as an impulse function.

This description of the creation of a compression shell by the microexplosion technique leads to a spring dampener control system, as presented schematically in Fig. 6(a), where the compression of the urethane chains is modeled by a spring,  $K$ , with a yield threshold,  $K_y$ , the viscous friction between the urethane chains is modeled as a dampener,  $B$ , and the mass of the the material originally in the void  $M$ . By making appropriate estimates for the constants we can use the force equation for the system

$$\frac{d^2y}{dt^2} = -\frac{B}{M} \frac{dy}{dt} - \frac{K[1 - K_y \text{Max}(y)]}{M} y(t) + f(t), \quad (1)$$

where the acceleration of the material in the system,  $d^2y/dt^2$ , is related to the force acting on the system,  $f(t)$ , and the internal reactions of the system. In order to solve this model, we re-write the equation using the Laplace transform for the Laplace operator  $s$ . This produces the transfer function

$$\frac{Y(s)}{F(s)} = \{Ms^2 + Bs + K[1 - K_y \text{Max}(y)]\}^{-1} \quad (2)$$

which characterizes a relation between the position of the mass,  $Y(s)$ , and the force applied to the system,  $F(s)$ , giving us the resulting impulse response. The impulse response describes the compression of the system which is then converted to permittivity, Fig. 6(b), with a slight modulation after the step is removed and replaced with the index of the unmodified polymer to simplify the calculations.

In our previous paper,<sup>18</sup> we have introduced another method of modeling the microexplosion fabricated structures. The applicability of the corresponding varying-index model was very limited, but it was able to account for the non removal of material from the system. The results obtained for this system are summarized

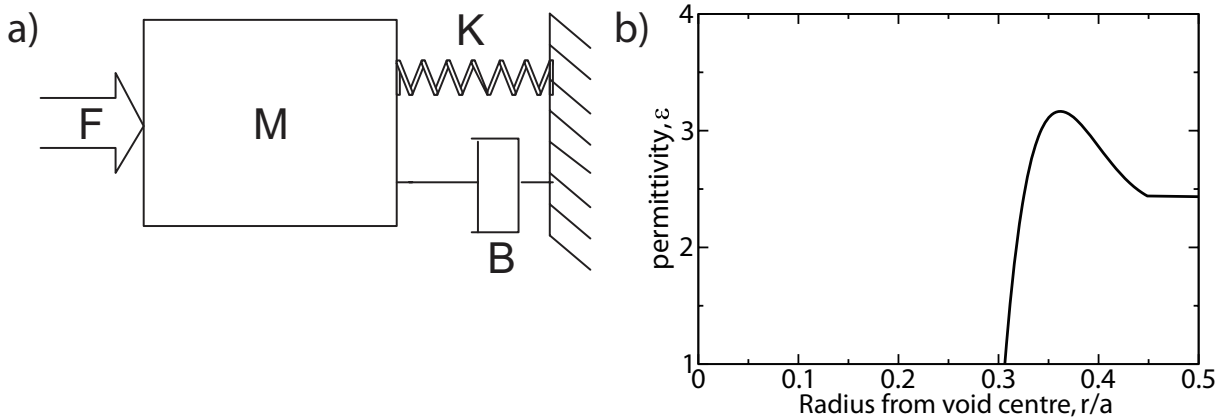


**Figure 6.** The image of the fabricated photopolymer crystal in Fig. 3 clearly shows a smooth change in the refractive index as you view the region near the wall of the hole. In (a) we see a control system which represents the compression,  $k$ , and dampening,  $b$ , force against the microexplosion,  $f$ , and also includes a relaxation force in response to the impact. Solving this system for an impulse (microexplosion) we obtain the resulting compression converted to permittivity shown in (b).

in Fig. 6(b) and they give us an upper limit for the possible frequency of the bandgap in the fabricated structure as well as the information about the frequency gap.

With the compression step model introduced above, we become aware of the limitations of our numerical approach to solving this problem. In order to solve Maxwell's equations, we employ the plane-wave method but like all numerical methods this requires sampling of the problem and measurement at specified points. In our model, this leads to a resonant cavity being formed which shifts the bandgap lower in the frequency. While for a single sample of the index step, Fig. 7(a), combined with the void and outer index, we expect a significant shift, the result with an increase in the sampling to 19 and then 114 points we see that the increase in smoothness does not correlate with an accuracy. This is due to the sampling of the numerical method which becomes our limiting factor. Even with very high sampling the resonance still maintains a bandgap frequency below that measured but approaches the experimental data.

In Fig. 7(b), the two bandgaps observed in the experimental data are bounded well by the respective bandgaps for the two models. The separation of the pair of bandgaps in each model relates well to the separation of the experimental results. When we consider the convergence in the compression step model towards higher values and the bounding limit of the varying index model we observe that both their midpoint [see Fig. 7(b)] presents a far better model for fitting the experimental data.

#### 4. DISCUSSIONS AND CONCLUSIONS

We have described above both the fabrication process and numerical modeling of the photonic structures created by using the microexplosion method in photopolymers. The microexplosion method is shown to be extremely suitable for the fabrication of photonic crystals. It allows to produce highly accurate photonic structures with the suppression of transmission as high as 75%. With the ease of this method and the large scale control the microexplosion high quality waveguides and other defect systems are far easier to fabricate than by applying other fabrication approaches. In addition, we have described the principles for introducing a new numerical model that accounts for the basic features of the microexplosion fabrication process; this model allows to explore quantitatively 3D photonic crystals created with this method.

Photopolymer photonic crystals fabricated by the microexplosion method have both advantages and disadvantages over their higher refractive index counterparts. We have seen that, the lower the refractive index, the higher the frequency of the bandgap. This allows photonic crystals to be produced for a given frequency of light with significantly larger features than their high index counterparts. Unfortunately, this advantage removes

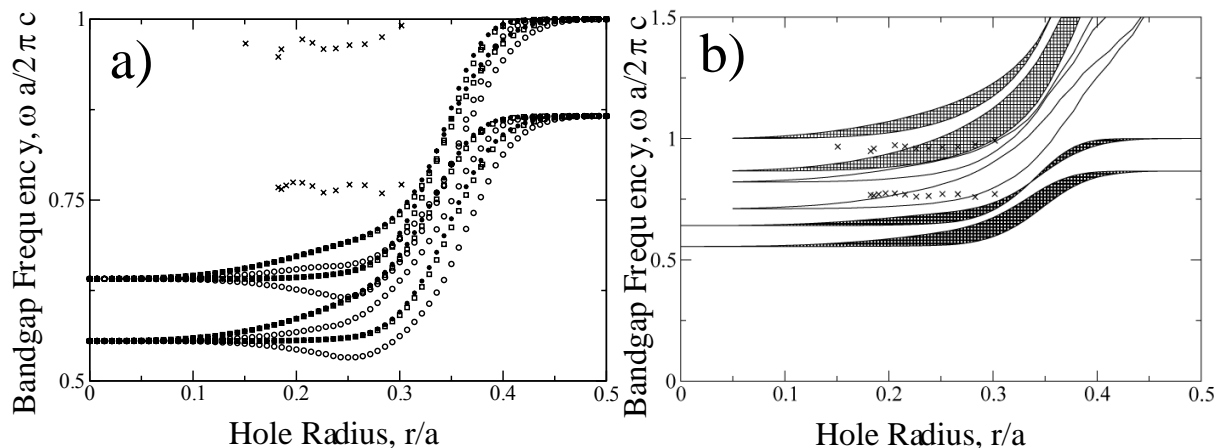


**Figure 7.** (a) The bandgap structure of the 3D fcc photonic crystal changes significantly when a smooth wall is implemented. In a single sample wall (bounded by circles), a large drop in the frequency is observed, but as the sampling is increased to 19 (bounded by squares) and 114 (bounded by stars) steps, we reach an asymptote where the frequency becomes static. This is due to resonances in the wall, which are exacerbated by discrete sampling. (b) Comparison between the 114 step (dark checkerboard) with the earlier varying index model (light checkerboard); the midpoint (black loop) bandgap provides a good match to the experimental data marked by crosses.

any possibility for such fundamental effects like all-angle negative refraction where the increased frequency leads to a larger free-space light cone removing a possibility for matching. Recently, the superprism effect has been observed in low-index photonic crystals,<sup>19</sup> and we may expect the observation other self-collimation related effects.

With this knowledge we can also predict that the effects of the infiltration of photonic crystals with liquid crystals and quantum dots within the system may produce significant nonlinear effects. With the high density of states at the bandgap edges we can foresee interesting applications to photonic-crystal laser fabrication including possibilities for low-threshold lasing and lasing outside of the frequency regions for currently available lasers. The key to all-optical devices will not be the result of one single fabrication method but a combination of different methods which are each advantageous for a specific task.

## ACKNOWLEDGMENTS

AM and YK thank Prof. C. Soukoulis for useful discussions and suggestions. This work was produced with the assistance of the Australian Research Council under the ARC Centers of Excellence Program. The Centre for Ultrahigh-bandwidth Devices for Optical Systems (CUDOS) is an ARC Centre of Excellence.

## REFERENCES

1. E. Glezer and E. Mazur, "Ultrafast-laser driven micro-explosions in transparent materials," *Appl. Phys. Lett.* **71**, p. 882, 1997.
2. K. Yamasaki, S. Juodkazis, M. Watanabe, H.-B. Sun, S. Matsuo, and H. Misawa, "Recording by microexplosion and two-photon reading of three-dimensional optical memory in polymethylmethacrylate films," *Applied Physics Letters* **76**(8), pp. 1000–1002, 2000.
3. D. Day and M. Gu, "Formation of voids in a doped polymethylmethacrylate polymer," *Appl. Phys. Lett.* **80**, p. 2404, 2002.
4. H.-B. Sun, Y. Xu, S. Matsuo, and H. Misawa, "Microfabrication and characteristics of two-dimensional photonic crystal structures in vitreous silica," *Opt. Rev.* **6**, p. 396, 1999.
5. H.-B. Sun, Y. Xu, S. Juodkazis, K. Sun, M. Watanabe, S. Matsuo, H. Misawa, and J. Nishii, "Arbitrary-lattice photonic crystals created by multiphoton microfabrication," *Opt. Lett.* **26**, p. 325, 2001.

6. H.-B. Sun, Y. Xu, K. Sun, S. Juodkazis, M. Watanabe, S. Matsuo, H. Misawa, and J. Nishii, "Inlaid 'atom'-like three-dimensional photonic crystal structures created with femtosecond laser microfabrication," *Proc. Mater. Res. Soc.* **605**, p. 85, 2000.
7. G. Zhou, M. J. Ventura, M. R. Vanner, and M. Gu, "Use of ultrafast-laser-driven microexplosion for fabricating three-dimensional void-based diamond-lattice photonic crystals in a solid polymer material," *Opt. Lett.* **29**, p. 2240, 2004.
8. M. Ventura, M. Straub, and M. Gu, "Void channel microstructures in resin solids as an efficient way to infrared photonic crystals," *Appl. Phys. Lett.* **82**, p. 1649, 2003.
9. G. Zhou, M. Ventura, M. Vanner, and M. Gu, "Fabrication and characterization of face-centered-cubic void dots photonic crystals in a solid polymer material," *Appl. Phys. Lett.* **86**, p. 011108, 2005.
10. M. Straub, M. Ventura, and M. Gu, "Multiple higher-order stop gaps in infrared polymer photonic crystals," *Phys. Rev. Lett.* **91**, p. 043901, 2003.
11. G. Zhou and M. Gu, "Anisotropic properties of ultrafast laser-driven microexplosions in lithium niobate crystal," *Appl. Phys. Lett.* **87**, p. 241107, 2005.
12. T. Trifonov, L. F. Marsal, A. Rodriguez, J. Pallars, and R. Alcubilla, "Analysis of photonic band gaps in two-dimensional photonic crystals with rods covered by a thin interfacial layer," *PHYS. REV. B* **70**, p. 195108, 2004.
13. V. Babin, P. Garstecki, and R. Holyst, "Multiple photonic band gaps in the structures composed of core-shell particles," *Journal of Applied Physics* **94**(7), pp. 4244–4247, 2003.
14. S. G. Romanov, A. S. Susha, C. M. S. Torres, Z. Liang, and F. Caruso, "Surface plasmon resonance in gold nanoparticle infiltrated dielectric opals," *Journal of Applied Physics* **97**(8), p. 086103, 2005.
15. R. Rengarajan, P. Jiang, V. Colvin, and D. Mittleman, "Optical properties of a photonic crystal of hollow spherical shells," *Applied Physics Letters* **77**(22), pp. 3517–3519, 2000.
16. K. P. Velikov, A. Moroz, and A. van Blaaderen, "Photonic crystals of core-shell colloidal particles," *Applied Physics Letters* **80**(1), pp. 49–51, 2002.
17. D. Day and M. Gu, "Effects of refractive-index mismatch on three-dimensional optical data-storage density in a two-photon bleaching polymer," *Appl. Opt.* **37**, p. 6299, 1998.
18. G. Zhou, M. Ventura, M. Gu, A. Matthews, and Y. Kivshar, "Photonic bandgap properties of void-based body-centered-cubic photonic crystals in polymer," *Opt. Express* **13**, p. 4390, 2005.
19. J. Serbin and M. Gu, "Experimental evidence for superprism effects in three-dimensional polymer photonic crystals," *Advanced Materials* **18**, p. 221, 2006.